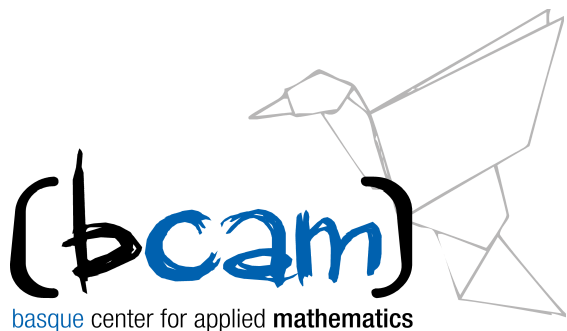


# The binormal flow, the Talbot effect, and non-circular jets

Luis VEGA, BCAM-UPV/EHU  
(with V. Banica and F. De la Hoz)



PDE zoom-seminar, Shanghai,  
Sept. 10, 2020



# Summary

(A) Binormal Flow (**BF**) a dispersive (geometric) PDE

- Critical regularity: Polygonal lines
- Selfsimilar solutions have finite energy ( $\widehat{L^2}_{\text{per}}$ )
- Talbot effect
- Continuation beyond the singularity time

(B) **BF** as a toy model in Fluid Mechanics: Vortex filament equation (**VFE**)

- Coherent structures are the self similar solutions
- Interaction: A weakly non-linear Talbot effect (**NLT<sub>e</sub>**)

Conjecture: **NLT<sub>e</sub>** can explain the turbulent dynamics of non circular jets

Q: **BF** for regular Polygons and regular polygonal helices

## (A) Binormal Flow

(BF) •  $\chi_t = \chi_s \wedge \chi_{ss} = cb$   $c$ : curvature  $b$ : binormal

(SM) •  $\chi_s = T$  Schrödinger map  $T_t = T \wedge T_{ss}$

(NLS) •  $\psi$  Hashimoto wave function 1d **NLS** (cubic focusing)

$\chi(0, s)$ : skew polygonal line

$T(0, s)$ : sequence of points  $T_j$  such that  $\lim_{j \rightarrow \pm\infty} T_j = A^\pm$

$$\psi(0, s) = \sum a_j \delta(s - j) \quad \sum_j |j|^{1+} |a_j|^2 < +\infty$$

$$\begin{pmatrix} T \\ e_1 \\ e_2 \end{pmatrix}_s = \begin{pmatrix} 0 & \alpha & \beta \\ -\alpha & 0 & 0 \\ -\beta & 0 & 0 \end{pmatrix} \begin{pmatrix} T \\ e_1 \\ e_2 \end{pmatrix}$$

$$\psi = \alpha + i\beta$$

# SCHRÖDINGER EQUATION

Hasimoto transformation:

$$\psi(s, t) = c(s, t) e^{i \int_0^s \tau(s', t) ds'}$$

$$c = c(s, t) \quad \text{curvature}$$

$$\tau = \tau(s, t) \quad \text{torsion}$$

$$\partial_t \psi(s, t) = i \left( \partial_s^2 \psi \pm \frac{1}{2} (|\psi|^2 + A(t)) \psi \right)$$

$$\int_{-\infty}^{\infty} |\psi(s, t)|^2 ds = \int_{-\infty}^{\infty} |\psi(s, 0)|^2 ds = \int_{-\infty}^{\infty} c^2(s, 0) ds$$

In our case

$$\psi(s, t) = \frac{a}{\sqrt{t}} e^{i \frac{s^2}{4t}} \quad , \quad \int_{-\infty}^{\infty} |\psi|^2 ds = +\infty.$$





# FLOW CONTROL WITH NONCIRCULAR JETS<sup>1</sup>

*E. J. Gutmark*

Mechanical Engineering Department, Louisiana State University, Baton Rouge,  
Louisiana 70803-6413; e-mail: gutmark@me.lsu.edu

*F. F. Grinstein*

Laboratory for Computational Physics and Fluid Dynamics, Code 6410,  
Naval Research Laboratory, Washington, DC 20375-5344;  
e-mail: grinstei@lcp.nrl.navy.mil

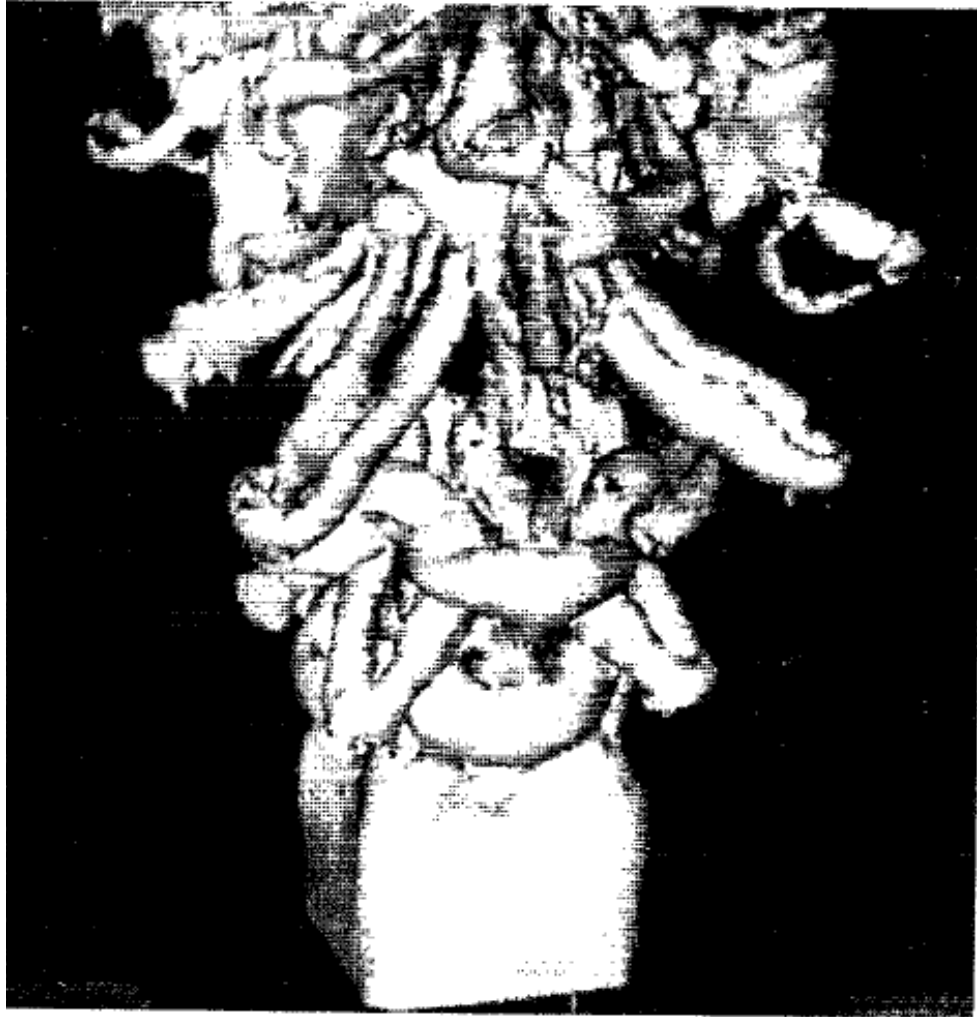
KEY WORDS: vortices, mixing, combustion, entrainment

---

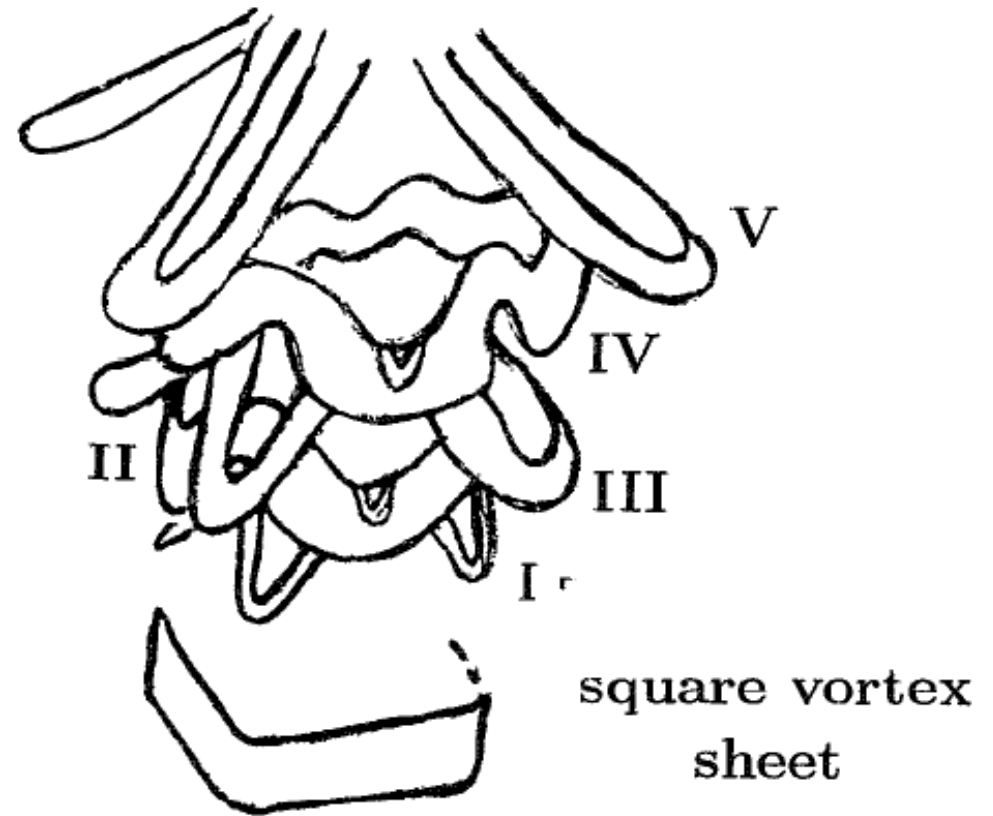
## ABSTRACT

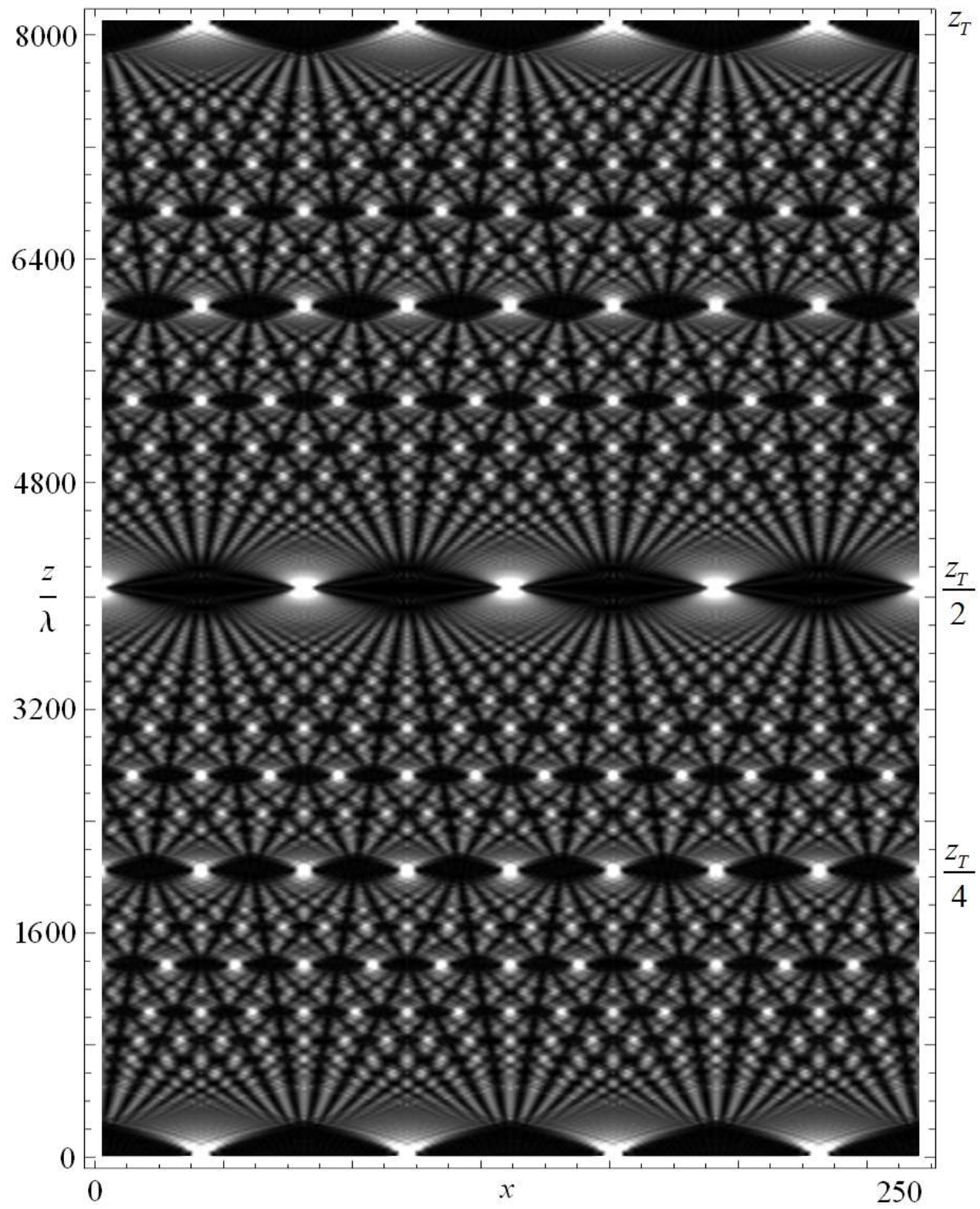
Noncircular jets have been the topic of extensive research in the last fifteen years. These jets were identified as an efficient technique of passive flow control that allows significant improvements of performance in various practical systems at a relatively low cost because noncircular jets rely solely on changes in the geometry of the nozzle. The applications of noncircular jets discussed in this review include improved large- and small-scale mixing in low- and high-speed flows, and enhanced combustor performance, by improving combustion efficiency, reducing combustion instabilities and undesired emissions. Additional applications include noise suppression, heat transfer, and thrust vector control (TVC).

The flow patterns associated with noncircular jets involve mechanisms of vortex evolution and interaction, flow instabilities, and fine-scale turbulence augmentation. Stability theory identified the effects of initial momentum thickness distribution, aspect ratio, and radius of curvature on the initial flow evolution. Experiments revealed complex vortex evolution and interaction related to self-induction and interaction between azimuthal and axial vortices, which lead to axis switching in the mean flow field. Numerical simulations described the details and clarified mechanisms of vorticity dynamics and effects of heat release and reaction on noncircular jet behavior.

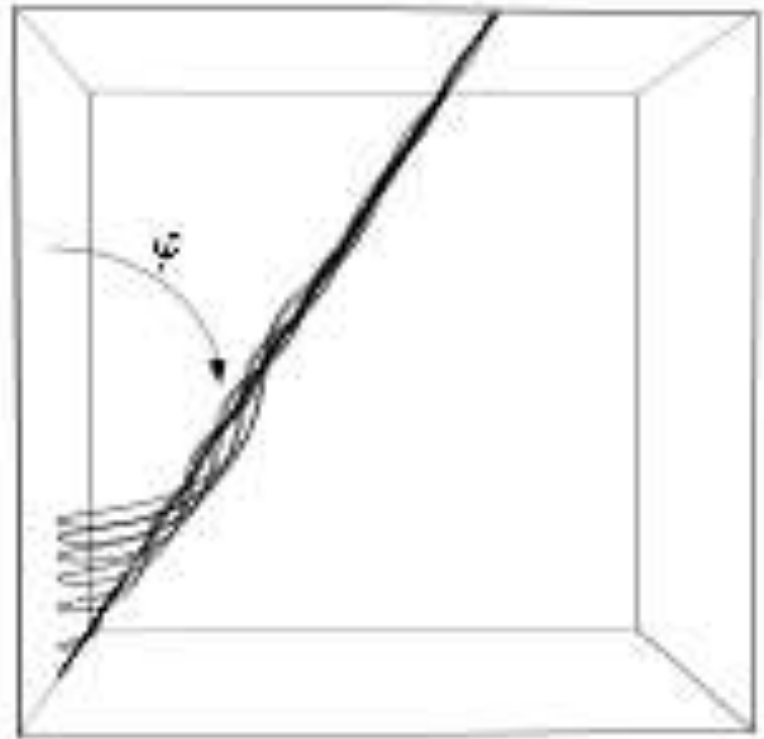
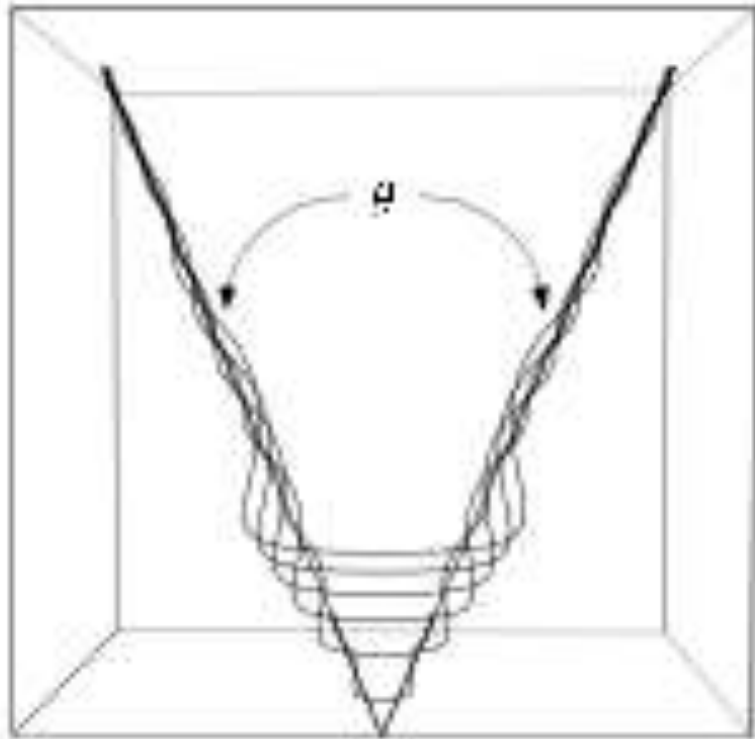


I, III, V : hairpin (braid) vortices  
II, IV : deformed vortex rings

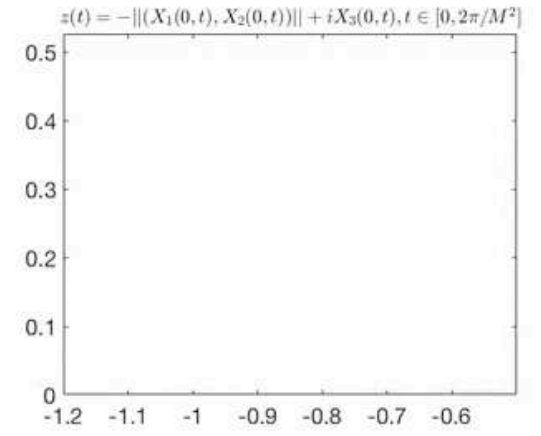
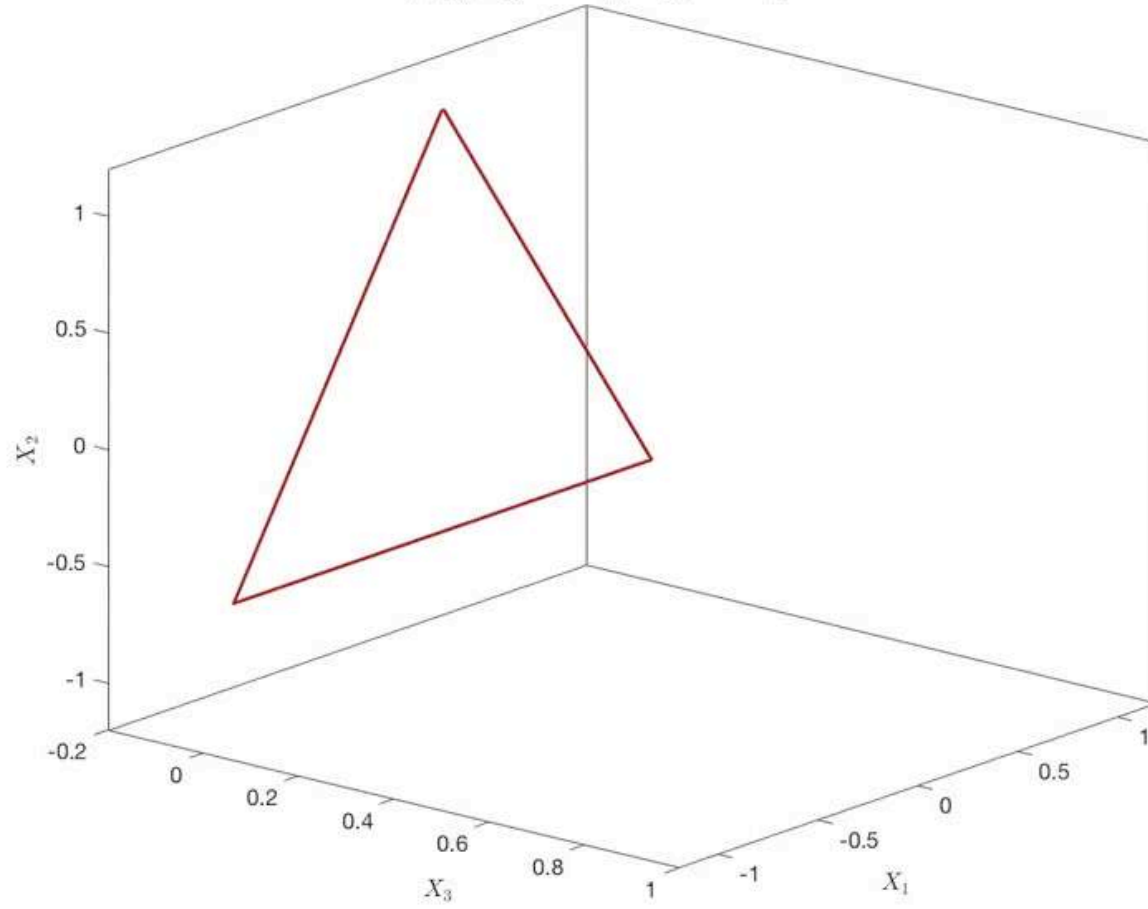




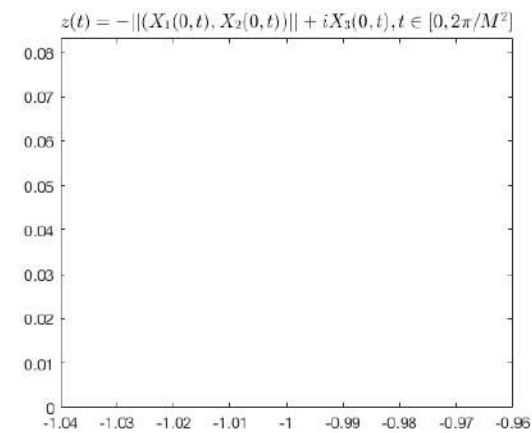
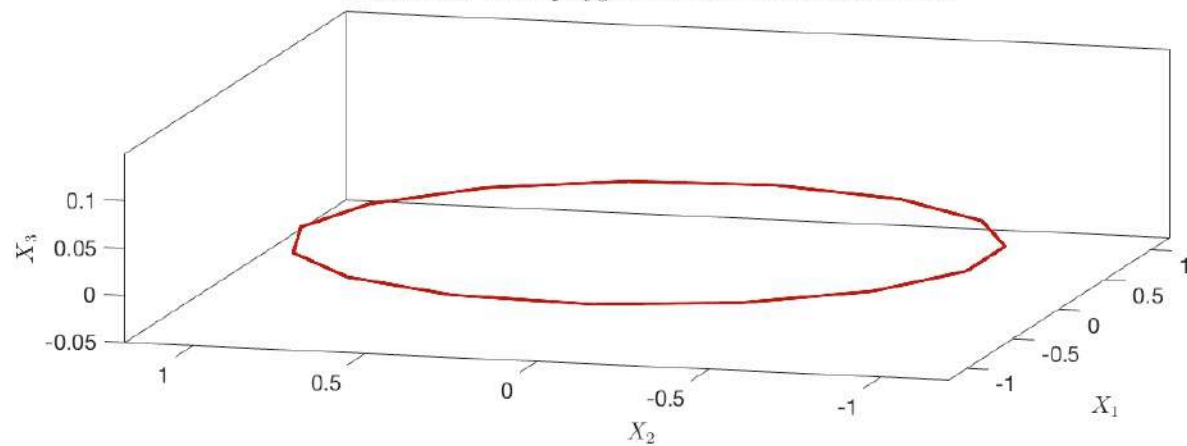




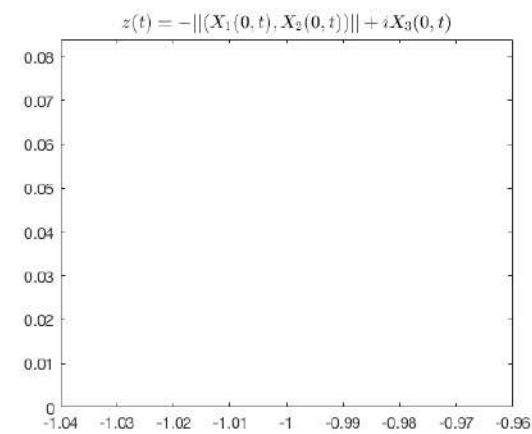
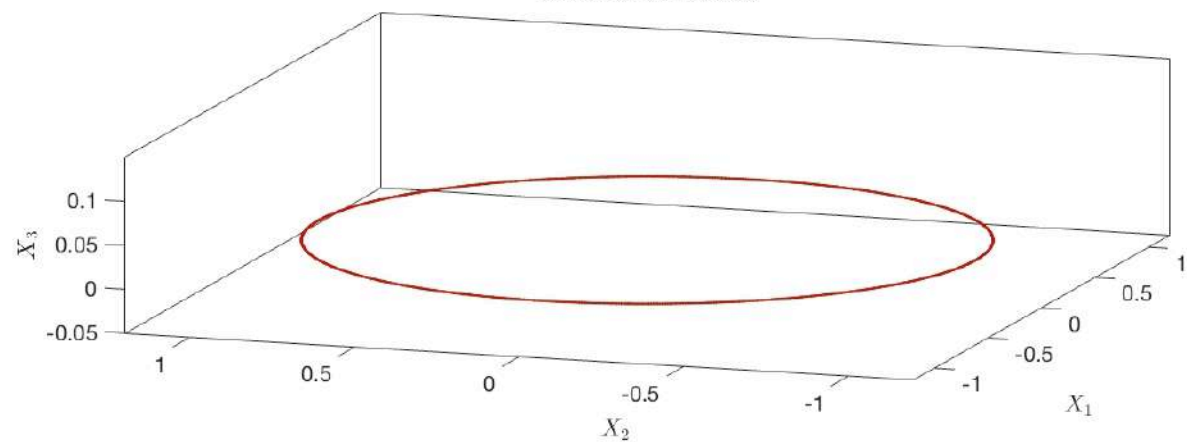
$X(s, t_{pq}) : t_{pq} = 2\pi.0/(M^2q), M = 3, q = 1260.$



Evolution of an  $M$ -polygon with zero torsion for  $M = 15$



Evolution of a circle



# Riemann's non-differentiable function

Integrating the Fourier series in time and evaluating at  $x = 0$  we get

$$\phi(t) = i \int_0^t u(0, \tau) d\tau = \sum_{k \in \mathbb{Z}} \frac{e^{-4\pi^2 ik^2 t} - 1}{-4\pi^2 k^2},$$

which is essentially Riemann's non-differentiable function.

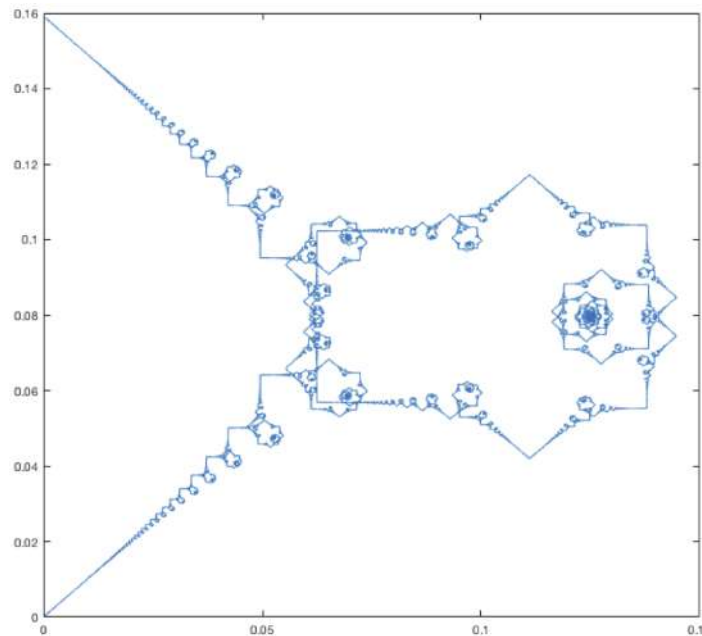
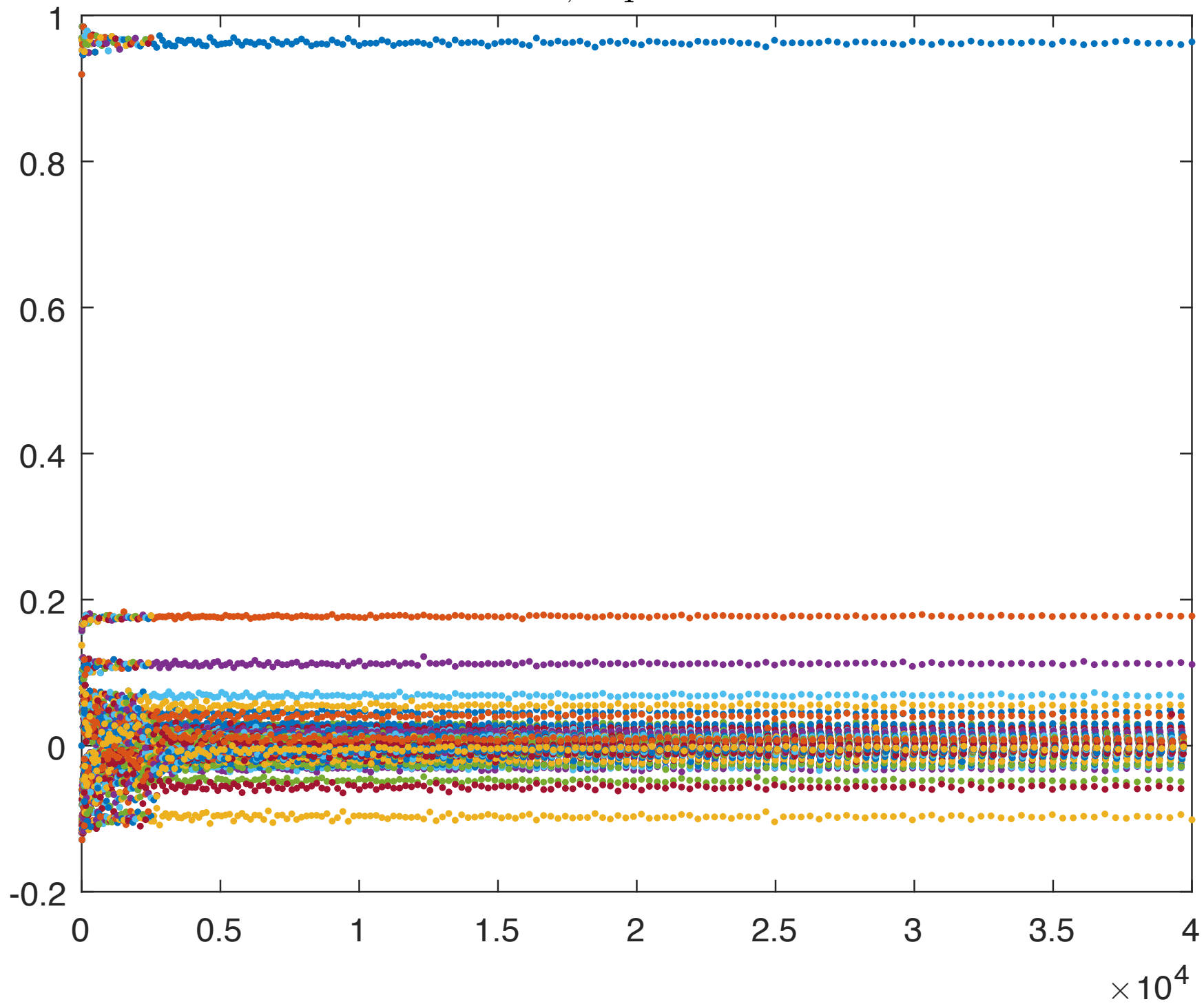
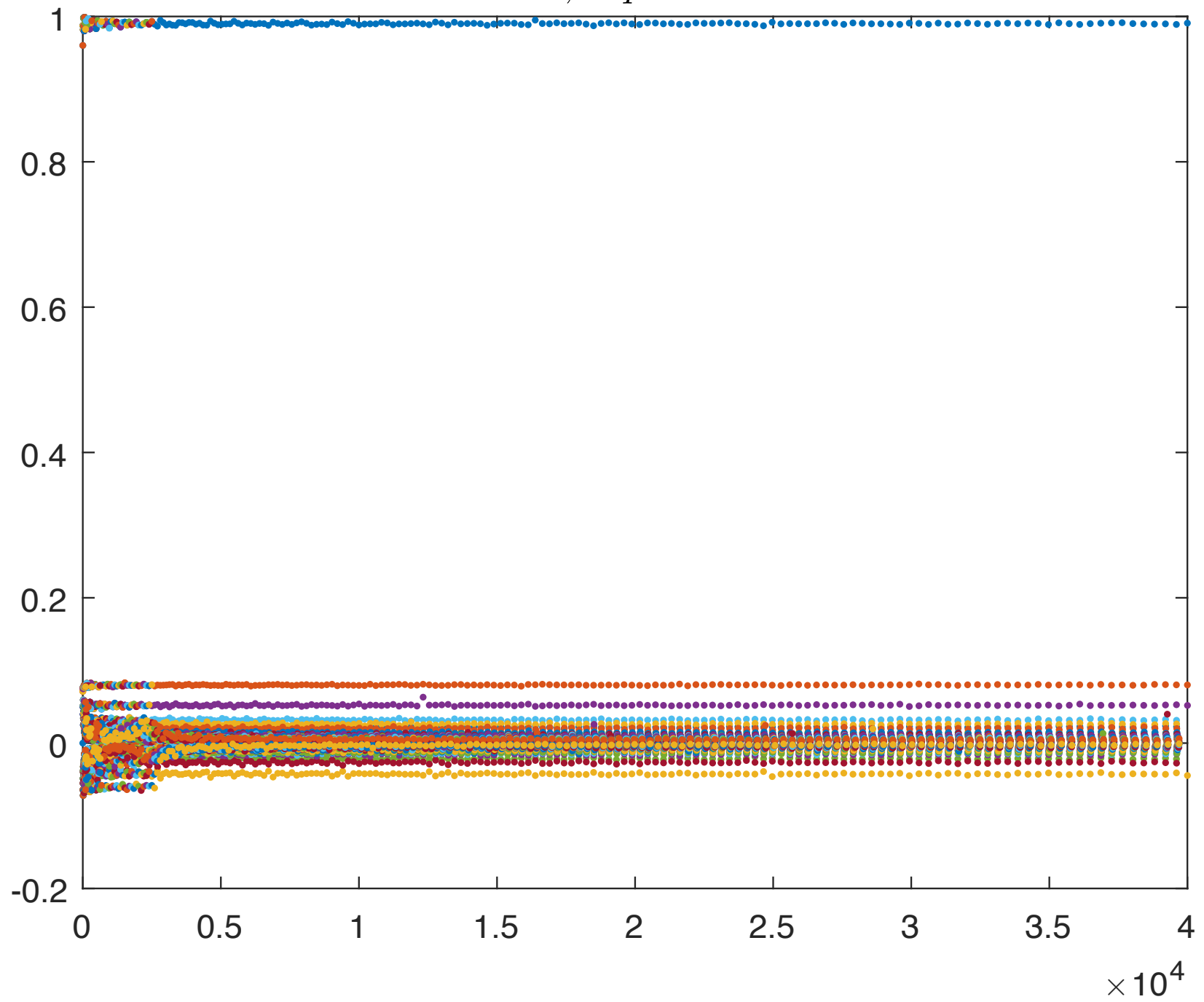


**Figure:** De la Hoz, Vega: *Vortex filament equation for a regular polygon*, *Nonlinearity* **27** (2014), 3031-3057

$M = 3, \quad q = 1048576$



$M = 4, \quad q = 1048576$



- Berry and Goldberg, Talbot Effect '88,
- Duistermaat '91,
- Oskolkov '92,
- Jaffard, multifractal '96,
- Kapitanski, Rodnianski '99,
- Olver '10
- Chen-Olver '12 '14; Olver-Sheils '17 Olver-Tsatis '18
- Jerrard-Smets '15,
- Erdogan-Tzirakis '13,
- De la Hoz-Vega '13, '17 critical regularity,
- Banica-Vega '18 critical regularity.

## (A) Binormal Flow

(BF) •  $\chi_t = \chi_s \wedge \chi_{ss} = cb$   $c$  : curvature  $b$  : binormal

(SM) •  $\chi_s = T$  Schrödinger map  $T_t = T \wedge T_{ss}$

(NLS) •  $\psi$  Hashimoto wave function 1d **NLS** (cubic focusing)

$\chi(0, s)$  : skew polygonal line

$T(0, s)$  : sequence of points  $T_j$  such that  $\lim_{j \rightarrow \pm\infty} T_j = A^\pm$

$$\psi(0, s) = \sum a_j \delta(s - j) \quad \sum_j |j|^{1+} |a_j|^2 < +\infty$$

$$\begin{pmatrix} T \\ e_1 \\ e_2 \end{pmatrix}_s = \begin{pmatrix} 0 & \alpha & \beta \\ -\alpha & 0 & 0 \\ -\beta & 0 & 0 \end{pmatrix} \begin{pmatrix} T \\ e_1 \\ e_2 \end{pmatrix}$$

$$\psi = \alpha + i\beta$$

# 1-D cubic NLS with several Dirac masses

We consider distributions

$$f = \sum_{k \in \mathbb{Z}} \alpha_k \delta_k.$$

Their Fourier transform on  $\mathbb{R}$  writes

$$\hat{f}(\xi) = \sum_{k \in \mathbb{Z}} \alpha_k e^{-ik\xi},$$

and in particular  $\hat{f}$  is  $2\pi$ -periodic. Imposing

$$\|\{\alpha_k\}\|_{l^{2,s}} := \sum_{k \in \mathbb{Z}} (1 + |k|)^{2s} |\alpha_k|^2 < \infty$$

translates into  $\hat{f} \in H^s(0, 2\pi)$ .

We define

$$H_{pF}^s := \{f \in \mathcal{S}'(\mathbb{R}), \hat{f}(x + 2\pi) = \hat{f}(x), \hat{f} \in H^s(0, 2\pi)\}.$$

## Result for 1-D cubic NLS with several Dirac data

**Theorem (Banica-V. 18).**— Let  $s > \frac{1}{2}$ ,  $0 < \gamma < 1$ ,  $\{\alpha_k\} \in l^{2,s}$  and  $M = \sum_{k \in \mathbb{Z}} |\alpha_k|^2$ .

We consider the 1-D cubic NLS renormalized equation:

$$i\partial_t u + \Delta u \pm \frac{1}{2}(|u|^2 - \frac{M}{2\pi t})u = 0.$$

There exists  $T > 0$  and a unique solution on  $(0, T)$  of the form

$$u(t, x) = \sum_{k \in \mathbb{Z}} e^{\mp i \frac{|\alpha_k|^2}{4\pi} \log t} (\alpha_k + R_k(t)) e^{it\Delta} \delta_k(x),$$

with

$$\sup_{0 < t < T} t^{-\gamma} \|\{R_k(t)\}\|_{l^{2,s}} + t \|\{\partial_t R_k(t)\}\|_{l^{2,s}} < C.$$

Moreover, if  $s \geq 1$  then the solution can be extended to  $(0, \infty)$ .

## Result for 1-D cubic NLS with several Dirac data

**Theorem**  $\star$  (**Banica-V. 18**).— Let  $a \in \mathbb{R}$ ,  $N \in \mathbb{N}$ ,  $M = \left(N - \frac{1}{2}\right) a^2$  and  $s > \frac{1}{2}$ .

We consider as initial data a finite sum of  $N$  Dirac masses with coefficients  $\alpha_k \in \mathbb{C}$  of equal modulus  $|\alpha_k| = a$ :

$$\begin{cases} i\partial_t u + \Delta u \pm \frac{1}{2} \left( |u|^2 - \frac{M}{2\pi t} \right) u = 0, \\ u(0) = \sum_k \alpha_k \delta_k. \end{cases}$$

There exists a unique global solution:

$$u(t) = e^{it\Delta} u(0) \pm ie^{it\Delta} \int_0^t e^{-i\tau\Delta} \left( \left( |u(\tau)|^2 - \frac{M}{2\tau} \right) u(\tau) \right) \frac{d\tau}{2},$$

such that  $e^{-it\Delta} \widehat{u}(t) \in \mathcal{C}^1(\mathbb{R}, H^s(0, 2\pi))$  with

$$\|e^{-it\Delta} u(t) - u(0)\|_{H_{pF}^s} \leq Ct^\gamma, \quad \forall t \in (-1, 1).$$

# Evolution of polygonal lines by the binormal flow

**Theorem (Banica-V. 18).**— Let  $\chi_0(x)$  be a polygonal line parametrized by arc length with corners located at  $x = k \in \mathbb{Z}$ , of angles  $\theta_k$  s.t.  $\{a_k\}$  defined by  $\sin(\frac{\theta_k}{2}) = e^{-\pi \frac{a_k^2}{2}}$  belongs to  $l^{2,3}$ . Then there exists  $\chi(t)$  smooth solution of the binormal flow on  $\mathbb{R}^*$ , solution in the weak sense on  $\mathbb{R}$  with

$$|\chi(t, x) - \chi_0(x)| \leq C\sqrt{t}, \quad \forall x \in \mathbb{R}, |t| \leq 1.$$

# Energy transfer

**Theorem.**– For  $t > 0$  we have the following conservation law:

$$\|T(t)\|_{L_{sc}^2}^2 = 4\pi \sum_j |\alpha_j|^2,$$

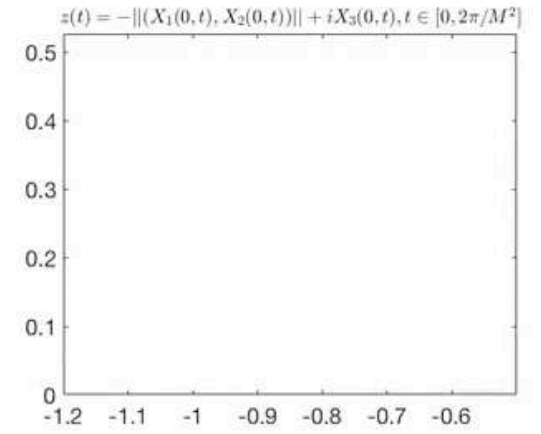
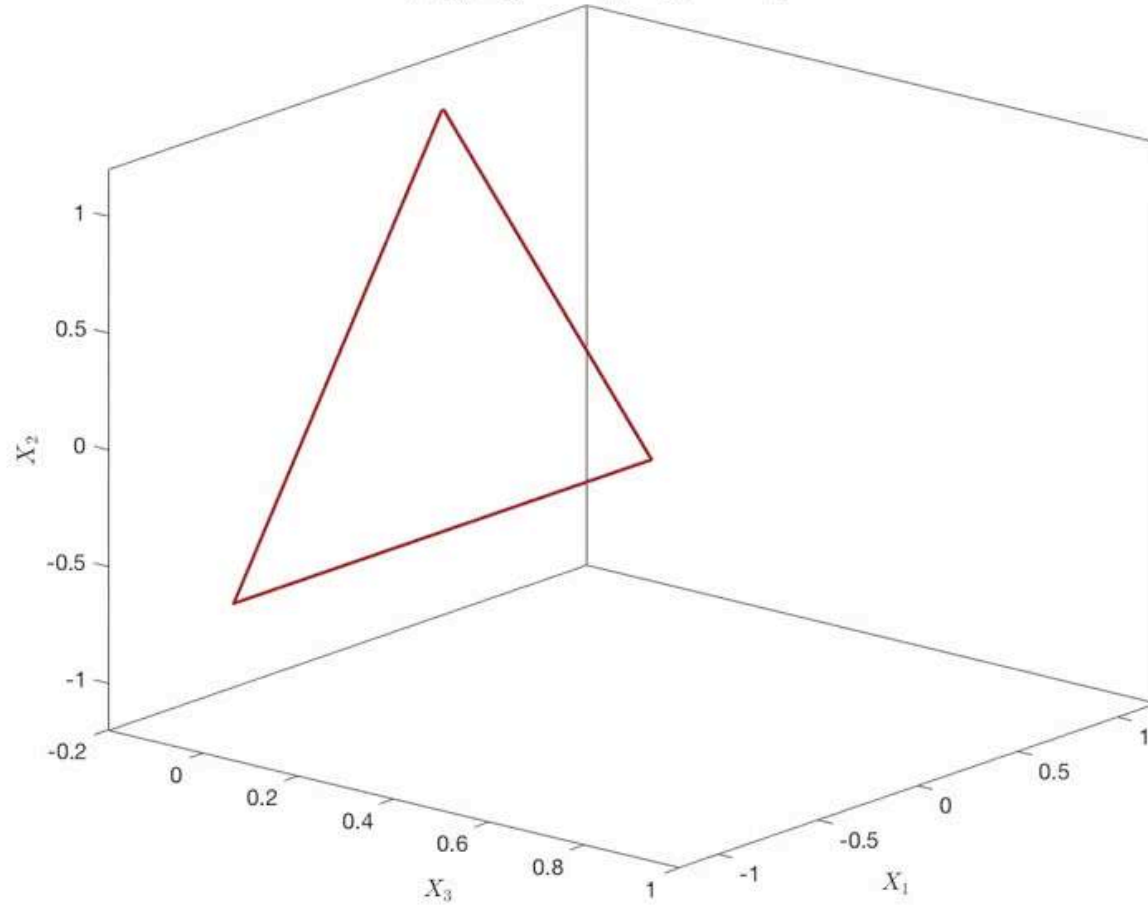
but

$$(*) \quad \|T(0)\|_{L_{sc}^2}^2 = 4 \sum_j (1 - e^{-\pi|\alpha_j|^2}),$$

where

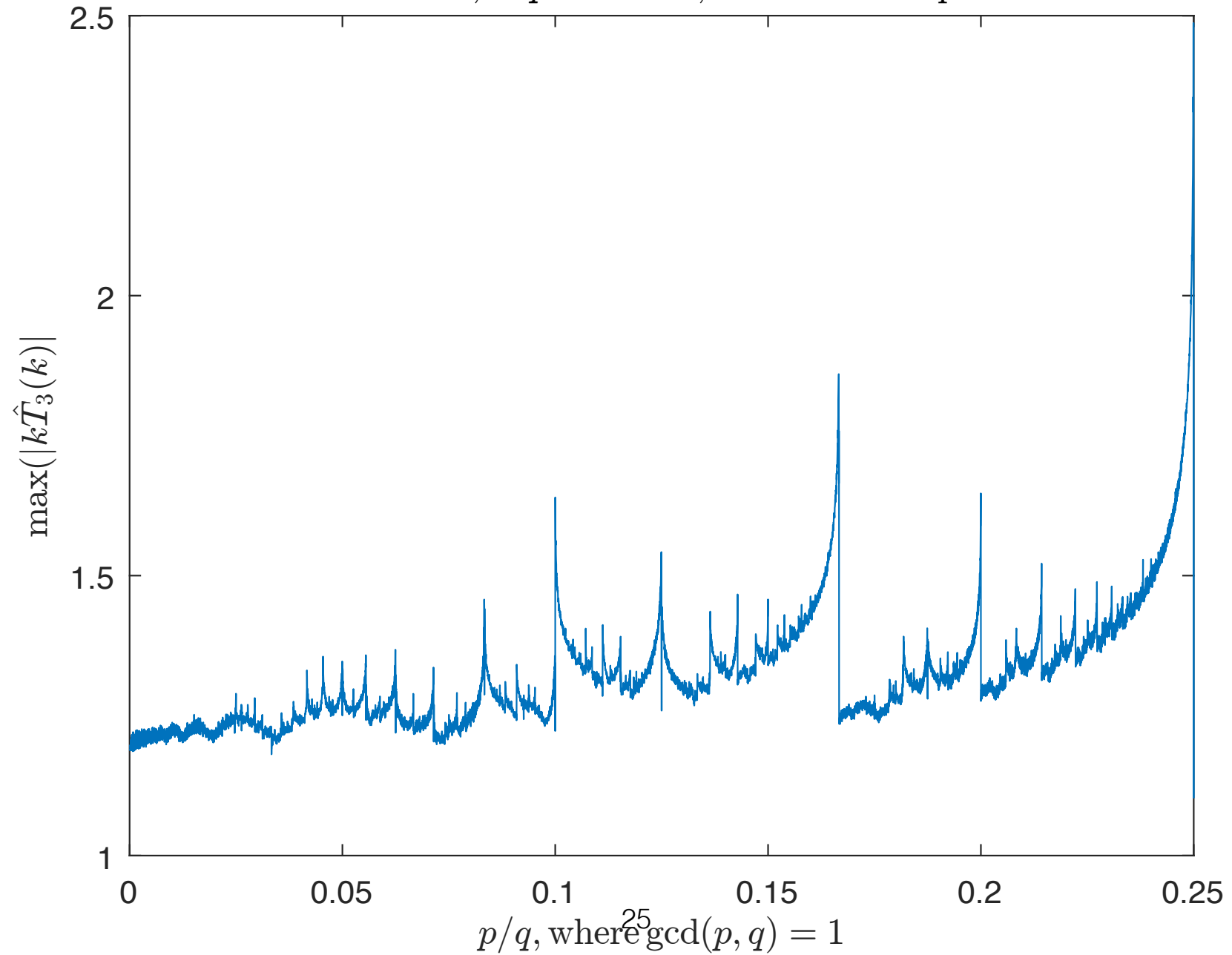
$$\|T(t)\|_{L_{sc}^2}^2 := \lim_{k \rightarrow \infty} \int_k^{k+1} |\widehat{T}_x(t, \xi)|^2 d\xi.$$

$X(s, t_{pq}) : t_{pq} = 2\pi.0/(M^2q), M = 3, q = 1260.$



# Energy Transfer, NLTe

$M = 3; \quad q = 120000; \quad 1920000 \text{ freq.}$



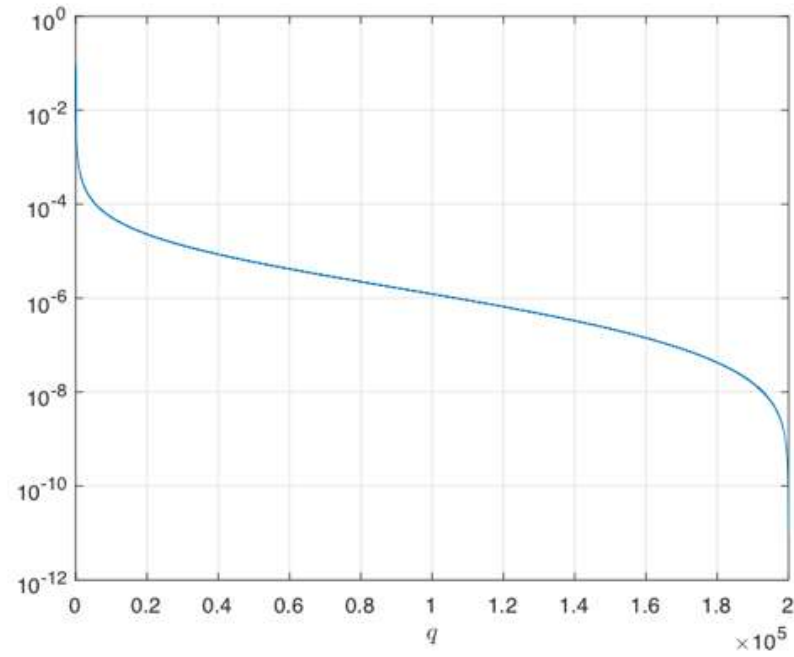


Figure 10:  $|\sqrt{2} \max_{t_{pq}} \|\widehat{T}_{1,s}(t_{pq})\|_{\infty} - a \ln(q) - b|$ , for  $a = 0.258039752572419$ ,  $b = 0.152992510344641$ .

**THANK YOU FOR YOUR  
ATTENTION**